Seasonal variability of multiple leaf traits captured by leaf spectroscopy at two temperate deciduous forests

Xi Yang[1,2], Jianwu Tang[2], John F. Mustard[1], Jin Wu[3], Kaiguang Zhao[4], Shawn Serbin[5], Jung-Eun Lee[1]

1. Department of Earth, Environment, and Planetary Sciences, Brown University, Providence, RI, 02912, USA
2. The Ecosystems Center, Marine Biological Laboratory, Woods Hole, MA, 02543, USA
3. Department of Ecology and Evolutionary Biology, University of Arizona, Tucson, AZ, 85721, USA
4. School of Environment and Natural Resources, Ohio Agricultural and Research Development Center, The Ohio State University, Wooster, OH 44691, USA
5. Environmental & Climate Sciences Department, Brookhaven National Laboratory, Upton, NY, 11973, USA

Keywords: phenology, leaf physiology, foliar chemistry, carbon cycle, chlorophyll, carotenoids, nitrogen, leaf mass per area, partial least square regression (PLSR), sun and shaded leaves

Corresponding authors:

Xi Yang, xi_yang@brown.edu; Jianwu Tang, jtang@mbl.edu.

Abstract

Understanding the temporal patterns of leaf traits is critical in determining the seasonality and magnitude of terrestrial carbon and water fluxes. However, robust and efficient ways to monitor the temporal dynamics of leaf traits are lacking. Here we assessed the potential of using leaf spectroscopy to predict leaf traits across their entire life cycle, forest sites, and light environments (sunlit vs. shaded) using a weekly sampled dataset across the entire growing season at two temperate deciduous forests. The dataset includes field measured leaf-level directional-hemispherical reflectance/transmittance together with seven important leaf traits [total chlorophyll (chlorophyll a and b), carotenoids, mass-based nitrogen concentration (N_{mass}), mass-based carbon concentration (C_{mass}), and leaf mass per area (LMA)]. All leaf properties, including leaf traits and spectra, varied significantly throughout the growing season, and displayed trait-specific temporal patterns. We used a Partial Least Square Regression (PLSR) analysis to estimate leaf traits from spectra, and found a significant capability of PLSR to capture the variability across time, sites, and light environment of all leaf traits investigated (R^2=0.6~0.8 for temporal variability; R^2=0.3~0.7 for cross-site variability; R^2=0.4~0.8 for variability from light environments). We also tested alternative field sampling designs and found that for most leaf traits, biweekly leaf sampling throughout the growing season enabled accurate characterization of the leaf trait seasonal patterns. Increasing the sampling frequency improved in the estimation of N_{mass}, C_{mass} and LMA comparing with foliar pigments. Our results, based on the comprehensive analysis of spectra-trait relationships across time, sites and light environments, highlight the capacity and potential limitations to use leaf

spectra to estimate leaf traits with strong seasonal variability, as an alternative to time-consuming traditional wet lab approaches.

1. Introduction

Leaf traits are important indicators of plant physiology (Wright et al. 2004), and critical components in numerous ecological processes (Kattge et al. 2011). For example, Leaf chlorophyll concentration represents the light harvesting potential and is related to photosynthetic activity (Niinemets 2007; Laisk et al. 2009), while accessory pigments such as carotenoids protect leaves from damage when exposed to excessive sunlight (Demmig-Adams and Adams 2000). Leaf mass per area (LMA) describes plants' investment to leaves in terms of carbon and nutrients to optimize sunlight interception (Poorter et al., 2009). Carbon is one of the major elements in cellulose and lignin, which are used to build the cell walls of various leaf tissues (Kokaly et al. 2009). Nitrogen is the key element in both carbon fixation enzyme RuBisCO and chlorophyll (Evans 1989), and thus plays an important role in modeling leaf and canopy photosynthesis (Bonan et al. 2012). The aforementioned leaf traits strongly depend on leaf developmental stages and light environments (Yang et al. 2014; Lewandowska and Jarvis 1977; Poorter et al. 2009; Wilson et al. 2000). Thus, capturing the spatial and temporal variations of these leaf traits is necessary to understand terrestrial ecosystem functioning (Schimel et al. 2015).

Despite the importance and increasing interests in the temporal and spatial variability of these (and many other) leaf traits, the capacity to monitor these traits over seasons has not progressed accordingly. Wet chemistry analysis of these leaf traits is considered to be the standard method, yet the destructive and time-consuming protocols do not allow for rapid and repeated sampling (including of the same leaves). On the other hand, field spectroscopy has shown promise in the augmentation of the traditional approaches (Asner and Martin 2008; Serbin et al. 2014). Despite this promise, many previous efforts that predict leaf traits using spectroscopy only focused on mature sunlit

leaves (e.g., Asner and Vitousek 2005; Ustin et al. 2004; Wicklein et al. 2012; but see Sims and Gamon (2002)) and have not explored the ability to track the continuous and developmental changes of leaf traits throughout the growing season. The temporal dimension of the spectra-trait relationship has mostly focused on leaf chlorophyll concentration (Belanger et al. 1995; Dillen et al. 2012; Shen et al. 2009), while it is largely unknown for other important leaf traits like nitrogen, carbon concentration and LMA. Moreover, the availability of high temporal resolution (~weekly) datasets on important leaf traits and spectra is limited. These data would be very useful for assessing the utility of leaf spectral properties (i.e. reflectance) for estimating the temporal variability of leaf traits, as well as scaling to broader regions and informing modeling activities.

Leaf traits not only change with time, but also with the light environments, such as the sun-lit or shaded light condition and the accompanying changes in microclimate, affect leaf traits (Ellsworth and Reich 1993; Niinemets, 2007), as a consequence of underlying fundamental evolutionary and ecophysiological constraints (Terashima et al. 2001). For example, shaded leaves display lower chlorophyll a to b ratio and higher LMA compared with sunlit leaves (Niinemets, 2007). As such, it is important to not only explore trait variation in space but also as in the vertical dimension to better capture ecosystem responses to global change.

Three categories of methods to estimate leaf traits from leaf spectral properties (i.e., reflectance and transmittance) are spectral vegetation indices (SVIs), statistical inversion methods exploiting the full wavelength (400 – 2500 nm), and leaf radiative transfer models like PROSPECT (Jacquemoud and Baret 1990), which are limited to a

few leaf traits and thus are not the focus of this study. SVIs are typically calculated using the reflectance from two or three wavelengths (Huete et al. 2002; Richardson et al. 2002; Sims and Gamon 2002). With proper calibration across a diverse range of vegetation types, SVIs can yield relatively robust models (Féret et al. 2011). While statistical methods such as Partial Least Square Regression (PLSR) modeling has become more popular in recent years with the availability of high-resolution spectra and increasing computational power (Asner and Martin 2008; Couture et al. 2013; Wold et al. 2001). Although both being widely used, these methods have not been thoroughly assessed, especially with respect to the robustness of PLSR models across time and different light environments (but see Serbin et al., 2014).

Here we aim to assess the ability of leaf optical properties to track temporal variability of a suite of leaf traits across sites and different light environments. We collected a dataset of ~weekly-sampled leaf traits [including total chlorophyll (and chlorophyll a and b), carotenoids, mass-based nitrogen concentration (N_{mass}), mass-based carbon concentration (C_{mass}), and LMA] along with *in situ* directional-hemispherical reflectance/transmittance during the growing season at two temperate deciduous forests. We first presented the temporal variations of leaf traits and spectra, and then highlight the ability of leaf spectra to track temporal variability of leaf traits. We investigate the robustness of the PLSR across season, sites, and growth environments. We further explore the optimal field sampling strategy. Finally, we conclude by discussing the broad implications of our study.

2. Study area and methods

2.1. Study sites

Our field sampling was conducted in two temperate deciduous forests located in the northeastern United States. The first site, on the island of Martha's Vineyard (MV, 41.362N, 70.578W), is a white oak (*Quecus alba*) dominated forest with a forest age of 80-115 years after natural recovery from abandoned cropland and pasture (Foster et al. 2002). Mean annual temperature is 10°C, and annual precipitation is about 1200 mm from 1981 to 2010 (Yang et al. 2014). Site 2, Harvard Forest (HF, 42.538N, 72.171W), has two dominating deciduous tree species: red oak (*Quercus rubra*) and red maple (*Acer rubrum*), with a few scattered yellow birch (*Betula alleghaniensis*). The forest age is 70-100 years. The annual mean temperature is about 7.5°C (Wofsy et al. 1993), and the annual precipitation is 1200 mm. Remote sensing studies suggested that the start of season in Martha's Vineyard is about 10-20 days later than that of HF (Fisher and Mustard 2007; Yang et al. 2012).

2.2. Measurements of leaf spectral properties and traits

We conducted two field campaigns to collect leaf traits at Martha's Vineyard and Harvard Forest. In 2011, weekly (biweekly in August) sampling of leaves throughout the growing season (June - November) was conducted at the Martha's Vineyard on three white oak trees. For each sampling period, we cut two fully sunlit branches (each having ~6 leaves) and one shaded branch using a tree pruner. The spectral properties of the leaves were immediately measured (see below). Then the leaves were placed in a plastic bag containing a moist paper towel, and all the samples were kept in a cooler filled with ice until being transferred back to the lab for further measurements. In 2012, the same weekly (biweekly from mid-July to late August) measurements in Harvard Forest were

made on five individuals (two red oaks, two red maples and one yellow birch) from May to October. For each tree, two sunlit and one shaded branch were collected each time.

Directional-hemispherical leaf reflectance and transmittance were measured immediately after the sampling using a spectroradiometer (ASD FS-3, ASD Inc. Boulder, CO, USA; spectral range: 300-2500 nm, spectral resolution: 3 nm@700 nm, 10 nm@1400/2100 nm) and an integrating sphere (ASD Inc.). The intensity of light source in the integrating sphere decreases sharply beyond 2200 nm, with the signal in 2200-2500 nm being noisy (ASD Inc., personal communications), and thus is excluded from the spectral-leaf traits analysis below.

The measured leaf traits include total chlorophyll concentration (including chlorophyll a and chlorophyll b, $\mu g/cm^2$), carotenoids ($\mu g/cm^2$), leaf mass per area (LMA, g/m^2), nitrogen concentration by mass (N_{mass}, %), and carbon concentration by mass (C_{mass}, %). Each branch was divided into two subsets. One subset was used to measure pigment concentrations. To measure the chlorophyll and carotenoids concentration, three leaf discs (~0.28 cm^2 each) were taken from each leaf using a hole puncher, and then ground in a mortar with 100% acetone solution and MgO (Asner et al. 2009). After an 8-minute centrifugation, the absorbance of the supernatant was measured using a spectrophotometer (Shimadzu UV-1201, Kyoto, Japan). Chlorophyll a, b and carotenoids concentrations were calculated using the readings from 470, 520, 645, 662 and 710 nm (Lichtenthaler and Buschmann 2001). The other subset (3 leaves) was scanned using a digital scanner (EPSON V300, EPSON, Long Beach, CA, USA), and oven-dried (65° C) for at least 48 hours for quantification of leaf dry mass. LMA was calculated based on the following equations:

$$LMA = W_{dry} / A_{leaf}$$

where W_{dry} is leaf dry mass weight, A_{leaf} is the leaf area calculated from the scanned leaf using ImageJ (Schneider et al. 2012). Dried leaves were then ground and analyzed for N_{mass} and C_{mass} with a CHNS/O analyzer (FLASH 2000, Thermo Scientific, Waltham, MA, USA).

2.3. Methods to estimate leaf traits using leaf spectral properties

We used two categories of methods to estimate leaf traits based on leaf spectral properties: vegetation indices that utilize the reflectance from two wavelengths, and statistical methods that exploit the information from the full leaf spectrum.

Based on extensive datasets from various types of biomes and plants, Féret et al. (2011) established polynomial relationships between SVIs and total chlorophyll concentration, carotenoids and LMA (Table 1). We also obtained the best estimate of a, b, and c using our own dataset (see below for the division between training and validation dataset).

Table 1 Simple Vegetation Indices (SVI) used in this study. These indices were calibrated using extensive datasets (Féret *et al.* 2011). Leaf traits were calculated based on a polynomial relationship: leaf trait = a × index^2 + b × index + c.

Leaf traits	Index	Coefficients		
		a	**b**	**c**
Chl ($\mu g/cm^2$)	$(R_{780}-R_{712})/(R_{780}+R_{712})$	40.65	121.88	-0.77
Car ($\mu g/cm^2$)	$(R_{800}-R_{530})/(R_{800}+R_{530})$	8.09	11.18	-0.38
LMA (g/cm^2)	$(R_{1368}-R_{1722})/(R_{1368}+R_{1722})$	-0.1004	0.1286	-0.0044

189 The second category of methods essentially is to build a multivariate linear
190 regression model(s) between leaf spectra and leaf traits (Zhao et al. 2013):

191 $$\mathbf{y} = \mathbf{X} \bullet \beta + \varepsilon$$

192 where **y** is an n-by-1 matrix of leaf traits (n equals to the number of leaf samples). **X** is an
193 n-by-m matrix (m equals the number of bands from each spectrum, and thus in this study
194 m=1800). ε is the n-by-1 estimation error that is to be minimized. PLSR modeling can be
195 used to develop the best model for the given dataset while avoiding over-fitting (Asner
196 and Martin 2008; Serbin et al. 2014). The numbers of independent factors used in the
197 regression were determined by minimizing the Prediction Residual Error Sum of Squares
198 (PRESS).

199 The above leaf traits and spectra (reflectance or transmittance) from two sites
200 were combined as one single dataset. To test the effectiveness of PLSR on this dataset,
201 the whole dataset is divided into two parts (70%-30%), for the training and validation of
202 PLSR, respectively. We used the Kennard-Stone algorithm to select the training subset
203 that provides a uniform coverage of the whole dataset (Kennard and Stone 1969). The
204 training dataset was used to optimize the regression model parameters (***β***), and then use
205 the validation dataset was used to test and evaluate the PLSR models. Evaluation
206 statistics include the R^2, Root Mean Square Error (RMSE) and normalized RMSE
207 (NRMSE), which is the RMSE divided by the range of the estimated leaf traits.
208 The relative importance of reflectance or transmittance at each wavelength is
209 determined by calculating the values of variable importance on projection (VIP) (Wold et
210 al. 2001). VIP is an indicator of the importance of each wavelength for the modeling of
211 both leaf traits (**y**) and spectra (**X**). Higher absolute values indicate greater importance of

212 the corresponding wavelength. Generally wavelengths with VIP value larger than 1 are
213 considered being important (Mehmood et al. 2012).
214
215 2.4. Robustness of PLSR models and scenarios for field sampling design
216 To examine the robustness of PLSR models across time, light environment, and
217 sites, we designed the following scenarios. In all the scenarios, we used leaf traits and
218 spectra of a subset of the whole dataset (e.g., leaf samples that are collected during only a
219 certain period of time, or a certain level of light environment) to build PLSR models, and
220 test the performance of the models against the remaining dataset.
221 For this we created five scenarios to examine how the timing of leaf sampling
222 affects predictability of seasonality of leaf traits. Leaf traits and spectra in the first three
223 scenarios were sampled only for the spring, summer, and fall, respectively. We defined
224 these three seasons based on variations in total chlorophyll concentration: days before
225 total chlorophyll reached a plateau in the mid-season were defined as spring; days when
226 total chlorophyll started to decrease were defined as fall; days between spring and fall
227 were defined as summer. The last two scenarios were that leaf traits and spectra were
228 sampled monthly or biweekly (instead of weekly as in the full dataset). We then use the
229 PLSR trained with leaf samples in the above scenarios to predict the leaf traits of the
230 entire dataset. There are two reasons to choose the whole dataset for validation: 1) the
231 whole dataset captures the temporal variability of leaf traits, which is the goal of this test;
232 2) it is necessary to have the same validation dataset to test the performance of these five
233 scenarios. Performance of these sampling strategies was measured by calculating the
234 RMSE and R^2.

We also explored our capacity to develop a generalized approach for capturing seasonality in leaf traits with spectral observations. Two tests were conducted to examine the robustness of PLSR models at different light environment and sites. Test 1 used sunlit leaf traits and spectra to train a PLSR model, which was then used to predict shaded leaf traits with corresponding spectra. We then switched the training and validation datasets so that shaded leaves were used to train PLSR model which sunlit leaves were used to validate. Test 2 divided the entire dataset into two subsets by geographic location: we used Martha's Vineyard dataset to calibrate the model, and Harvard Forest dataset to validate, and vice versa.

3. Results

3.1. Temporal and spatial variability of leaf traits

All leaf traits displayed significant temporal variations throughout the growing season (Fig.1 and 2). Overall, pigments from both sites have similar bell-shaped trajectories, despite being sampled from different species and locations within the canopy. Chlorophyll and carotenoids concentration rapidly increased from ~10 $\mu g/cm^2$ at the beginning of the season, and then stabilized around ~50 $\mu g/cm^2$ and ~40 $\mu g/cm^2$ in Martha's Vineyard and Harvard Forest respectively during the summer followed by a decline in the fall to 10 $\mu g/cm^2$ before leaf shedding. The Harvard Forest samples were from three different species, and showed much larger variability compared with Martha's Vineyard, especially for the shaded leaves (Fig.1 e-h). The carotenoids concentration was ~3 $\mu g/cm^2$ at the beginning/end of the season and ~10 $\mu g/cm^2$ at the peak season. The total chlorophyll concentration relative to the carotenoids concentration (Chl/Car) increased during the early seasons. In the fall, though both chlorophyll and carotenoids

258 decreased, Chl/Car decreased steadily, as a result of faster decline of chlorophyll relative
259 to the carotenoids (Fig. S1a).

260

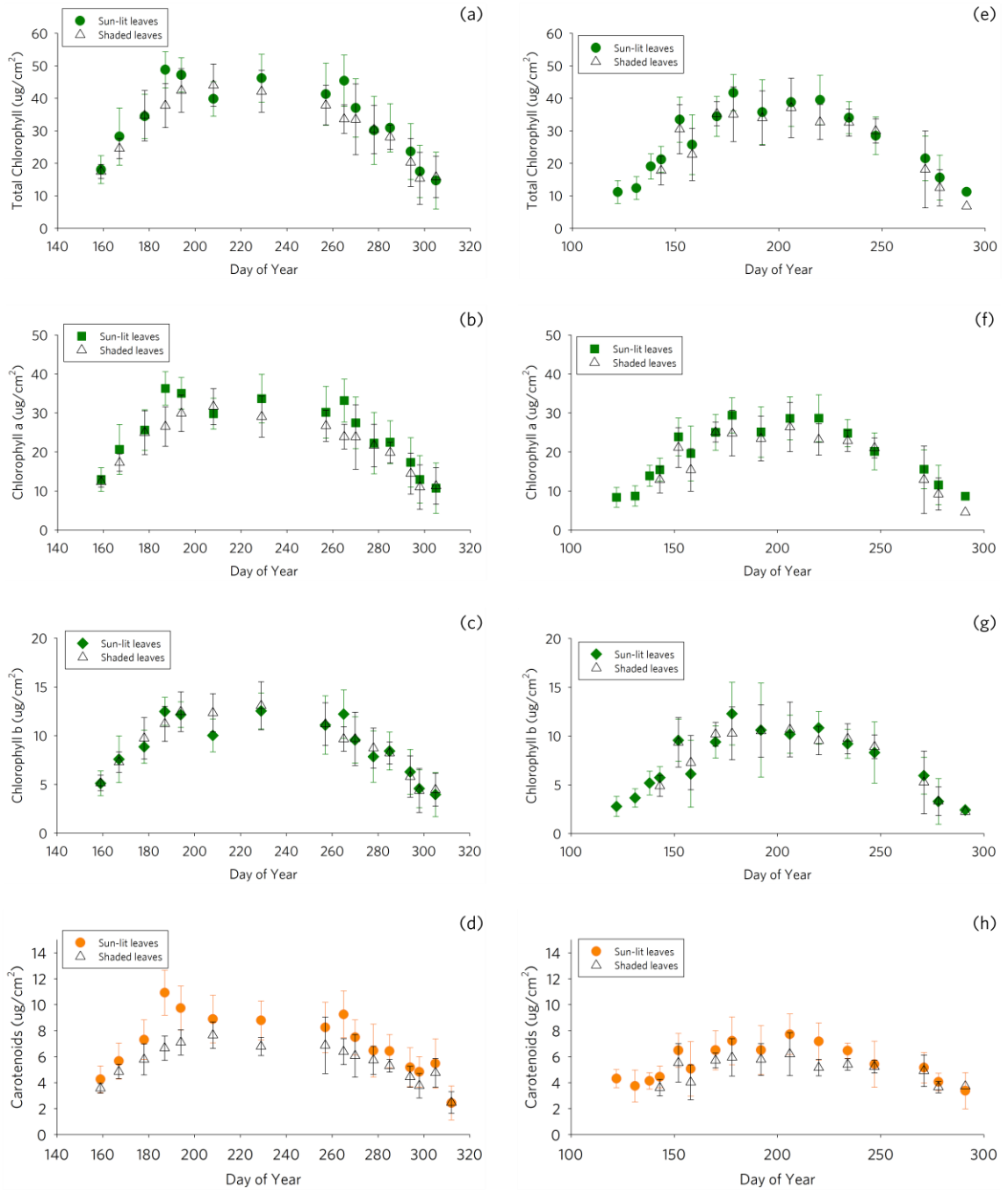

261

262 **Figure 1** Seasonal patterns of pigments of sunlit (diamonds) and shaded (open triangles)
263 leaves from two deciduous forests. Martha's Vineyard, year 2011: (a) Total chlorophyll;

(b) chlorophyll a; (c) chlorophyll b; (d) carotenoids. Harvard Forest year 2012: (e) Total chlorophyll; (f) chlorophyll a; (g) chlorophyll b; (h) carotenoids. Each dot is the mean value of all the samples collected that day. Error bars are standard deviations.

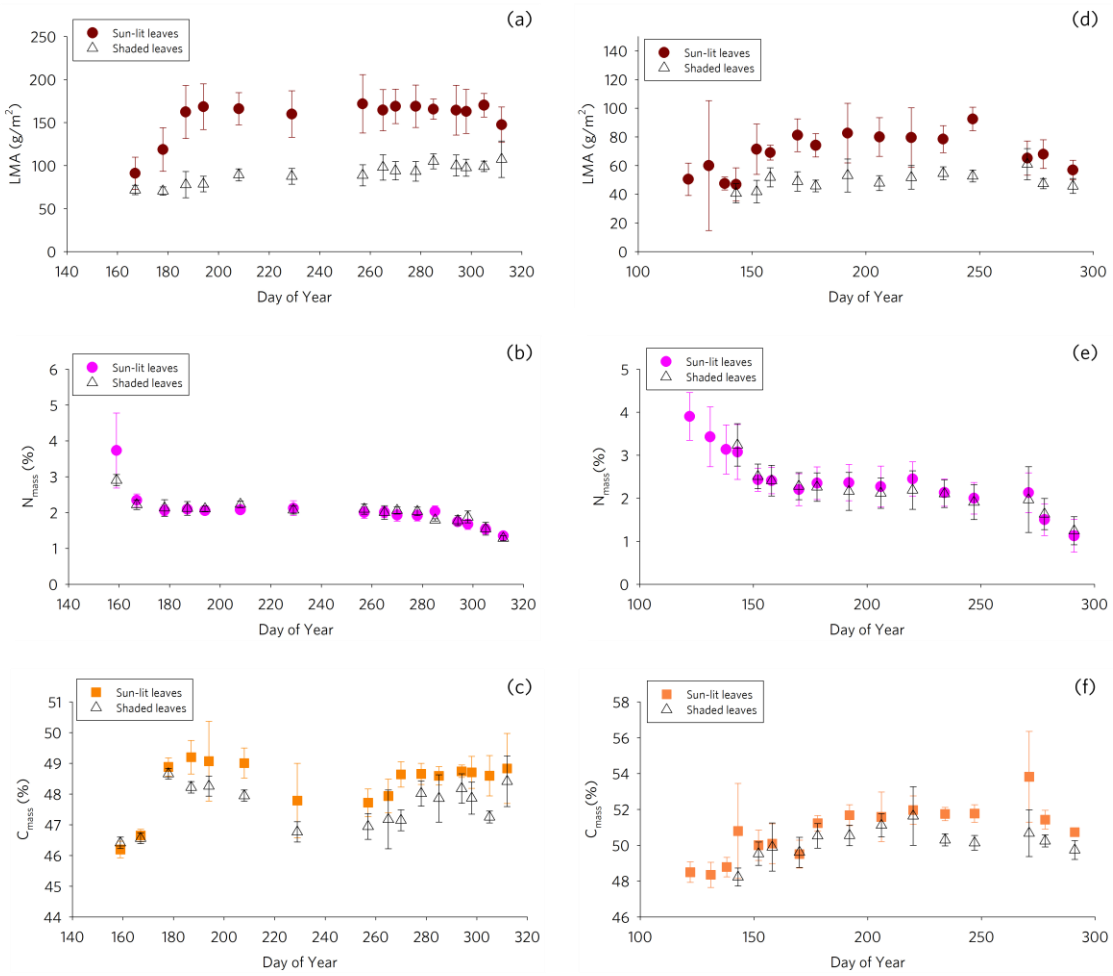

Figure 2 Seasonal patterns of biochemical and biophysical properties of sunlit (closed symbols) and shaded (open symbols) leaves from two deciduous forest sites. Martha's Vineyard, year 2011: (a) Leaf mass per area (LMA); (b) mass-based nitrogen concentration (N_{mass}); (c) mass-based carbon concentration (C_{mass}). Harvard Forest, year 2012: (d) LMA; (e) N_{mass}; (f) C_{mass}. Each dot is the mean value of all the samples collected that day. Error bars are standard deviations.

The remaining three leaf traits (LMA, N_{mass}, and C_{mass}) displayed different seasonal patterns compared with leaf pigments (Fig. 2). For example, LMA rapidly increased in the spring, but showed only a minor decline by the end of the measurement

period. N_{mass} was higher (~4-5%) at the start of the season, and remained stable around 2% during the summer, followed by ~1% decrease in the fall, presumably caused by nitrogen resorption (Eckstein et al. 1999). Similar to LMA, C_{mass} accumulated 2-4% in the spring and stabilized for the rest of the growing seasons around 50%. The rapid increase of LMA in the spring was accompanied by a similar increase of C_{mass} and decrease of N_{mass}, which all ended at the same time (DOY ~194 in Martha's Vineyard, and DOY ~170 in Harvard Forest).

Mean annual values of leaf traits from Martha's Vineyard were significantly different from those at Harvard Forest (Table 2). For example, leaf chlorophyll in Martha's Vineyard is 5.64 $\mu g/cm^2$ (17.5%) higher than that from Harvard Forest ($p < 0.0001$). LMA in Martha's Vineyard showed much larger variation than that from Harvard Forest, and the mean LMA was 39.85 g/m^2 (37.5%) higher than that from HF. Similar situation applies to all other leaf traits except for C_{mass}, for which value at HF were higher than the traits at MV.

Sunlit leaves contained more total chlorophyll and carotenoids (Fig. S2) and the carotenoids to the total chlorophyll ratio was significantly higher for sun-lit leaves comparing with shaded leaves (Martha's Vineyard, $p < 0.0001$; Harvard Forest, $p = 0.0182$). Chlorophyll a/b was also significantly larger for sunlit leaves in both sites (MV, $p < 0.0001$; HF, $p < 0.0001$). Similarly, LMA and C_{mass} values were significantly higher in the sun-lit leaves versus shaded foliage, with the only exception of N_{mass}, in which both sun-lit and shaded leaves were indistinguishable throughout the two seasons (Fig. 2b).

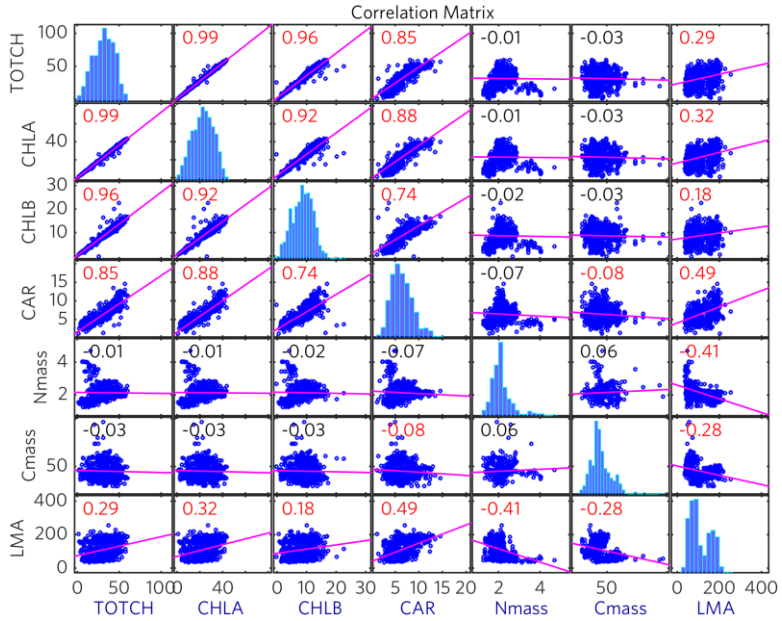

299

300 **Figure 3** Correlation matrix of all the leaf traits. Histograms of each leaf traits are on the
301 diagonal positions. Number on each subplot indicates R^2 (Red means $p<0.05$). See Table
302 2 for units.

303 **Table 2** Annual mean values and standard deviation of leaf traits at two sites (stars
304 indicate the p-values of t-test between the values of leaf traits from two sites: ***:
305 $p<0.0001$; **: $p<0.01$; *: $p<0.05$).

Leaf traits	Units	MV	HF
Total Chl ($\mu g/cm^2$)***	$\mu g/cm^2$	31.74 (12.17)	26.19 (9.29)
Chl a ($\mu g/cm^2$)**	$\mu g/cm^2$	23.19 (8.81)	18.92 (6.70)
Chl b ($\mu g/cm^2$)**	$\mu g/cm^2$	8.70 (3.31)	7.48 (2.73)
Car ($\mu g/cm^2$)**	$\mu g/cm^2$	6.16 (2.28)	5.59 (1.33)
N_{mass} (%)**	% (unitless)	2.17 (0.50)	2.03 (0.50)
C_{mass} (%)***	% (unitless)	48.34 (1.24)	51.12 (0.87)
LMA (g/cm^2)***	g/m^2	106.29 (45.04)	66.44 (15.56)

306

A linear regression analysis highlighted various levels of correlation among leaf traits (Fig. 3). Close correlation was found among leaf pigments: total chlorophyll concentration was highly correlated with carotenoids concentration (R^2 = 0.85), suggesting a tight coupling among those pigments throughout the growing season despite the faster decrease of chlorophyll concentration during the senescence (Fig. S1). For the entire dataset (across all sunlit and shaded leaves from different species), N_{mass} was weakly correlated with pigments. LMA showed positive correlation with all pigments while a negative correlation was observed with N_{mass} and C_{mass}.

3.2. Seasonal variability of leaf spectral properties

The full leaf reflectance and transmittance spectrum showed significant variability in both amplitude and shape (Fig.4). The visible (VIS, 400 – 700 nm) and near infrared (NIR, 700-1000 nm) changed dramatically throughout the season, while shortwave infrared (SWIR, 1000-2500 nm) was relatively stable. Data from Martha's Vineyard showed larger variability in NIR compared to Harvard Forest.

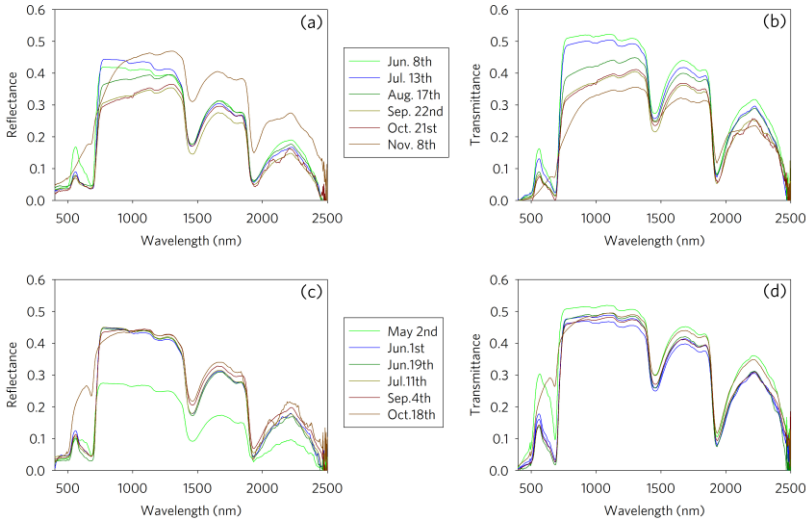

Figure 4 Examples of leaf directional-hemispherical reflectance and transmittance measured on (a, b) Martha's Vineyard and in (c,d) Harvard Forest.

Fig.S3 shows the seasonal variations of individual bands. The R, G, and B reflectance at both sites showed a U-shape pattern (Fig. S3a, S3c): all of them decreased in the beginning of the season; and increased in the end of the season after a stable summer. The NIR from Martha's Vineyard showed a consistent decline in the mid-summer and then increased in the fall, while the NIR from Harvard Forest was relatively stable throughout the season. Leaf transmittance at each band had similar patterns as the reflectance (Fig. S3b, S3d).

3.3. Comparisons of methods of leaf traits estimation

We compared two categories of methods to estimate leaf traits from leaf spectra. Overall, PLSR consistently outperformed the SVIs in estimating leaf traits, showing an improved performance when the SVIs were trained by the original datasets or our own dataset (Table 3). The PLSR models using leaf reflectance ($PLSR_{ref}$ hereafter) had slightly better performance compared with those using leaf transmittance ($PLSR_{tra}$

hereafter) when assessed with the independent dataset. For different leaf traits, the performance of these methods varied, as described in details below.

Leaf chlorophyll from the validation dataset was well estimated by $PLSR_{ref}$ (Fig.5. $R^2 > 0.70$ and NRMSE < 10%). The SVI for chlorophyll showed slightly larger prediction error (0.5 $\mu g/cm^2$) compared with $PLSR_{ref}$ and $PLSR_{tra}$ (Table 3). The two components of chlorophyll (chl a and b) were also well captured by the $PLSR_{ref}$ approach with NRMSE less than 10% and R^2 of 0.73 and 0.66 respectively. Similarly, carotenoids were estimated relatively well by $PLSR_{ref}$ and $PLSR_{tra}$ (R^2 >0.65) but the SVI for carotenoids had higher 30% higher RMSE comparing with $PLSR_{ref}$.

N_{mass} was well captured by leaf spectra especially with the reflectance dataset (Fig.5. $R^2 > 0.6$ and NRMSE < 5%). Similarly, both $PLSR_{ref}$ and $PLSR_{tra}$ explained ~60% of the variance in C_{mass} ($R^2 > 0.6$ and NRMSE < 7%). PLSR also displayed a strong capacity to predict LMA (R^2 = ~0.80 and NRMSE < 9%), where the SVI for LMA could not capture more than 20% of the variation in LMA and more than double the RMSE of $PLSR_{ref}$ mainly due to a saturation effect (data not shown).

Table 3 Comparisons among methods in terms of the goodness-of-fit (RMSE, NRMSE and R^2) for the dataset at both Martha's Vineyard and Harvard Forest. $PLSR_{ref}$ indicates models using reflectance dataset to predict leaf traits. $PLSR_{tra}$ indicates models using transmittance dataset to predict leaf traits.

Leaf traits	RMSE (NRMSE)				R^2			
	Simple indices (Féret *et al.* 2011)	Simple indices (this dataset)	$PLSR_{ref}$	$PLSR_{tra}$	Simple indices (Féret *et al.* 2011)	Simple indices (this dataset)	$PLSR_{ref}$	$PLSR_{tra}$
Total Chl ($\mu g/cm^2$)	5.93	6.04	5.48 (0.09)	5.62 (0.10)	0.71	0.71	0.73	0.64
Chl a ($\mu g/cm^2$)			3.99 (0.09)	4.14 (0.09)			0.73	0.68
Chl b ($\mu g/cm^2$)			1.62 (0.07)	1.82 (0.08)			0.66	0.58
Car ($\mu g/cm^2$)	1.53	1.54	1.07 (0.08)	1.20 (0.09)	0.39	0.40	0.71	0.68
N_{mass} (%)			0.22 (0.05)	0.24 (0.05)			0.63	0.54
C_{mass} (%)			0.93 (0.07)	0.95 (0.07)			0.63	0.71
LMA (g/cm^2)	40.6	39.7	18.11 (0.08)	19.01 (0.09)	0.20	0.19	0.85	0.79

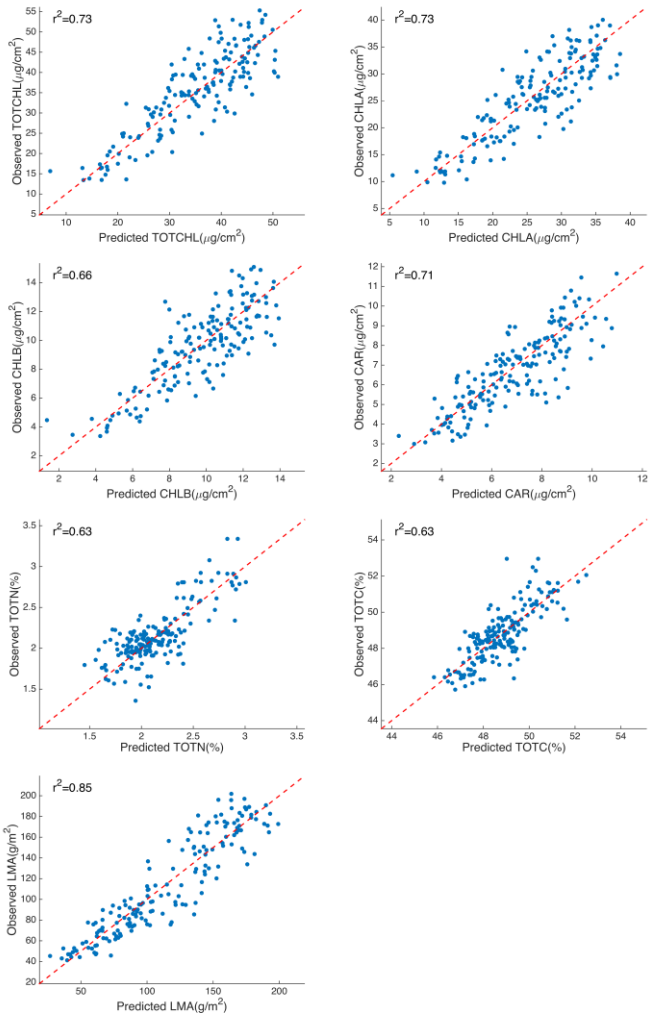

358

359 **Figure 5** Comparisons between the observed leaf traits and predicted traits from $PLSR_{ref}$.
360 For detailed statistics refer to Table 2 and 3. Observations are from the independent
361 validation dataset selected using the Kennard-Stone method. The red dashed lines are 1:1
362 line.

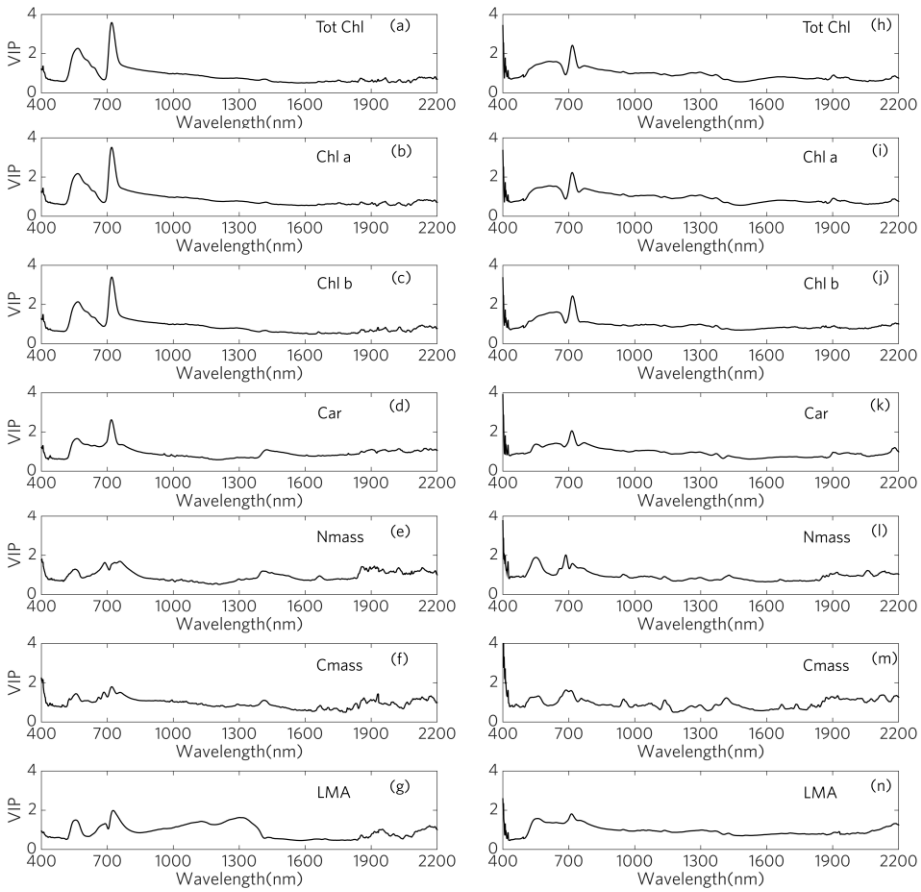

Figure 6 Relative importance of each wavelength in Variable Importance on Projection (VIP). VIP values from $PLSR_{ref}$ and $PLSR_{tra}$ are on the right and left, respectively.

The VIP values of PLSR show the relative importance of each wavelength in predicting leaf traits (Fig.6). Visible and near-infrared wavelengths were important to the prediction of leaf pigments; there are three peaks (400, 550 and 730 nm) that are related to the chlorophyll absorption in the red (620-750 nm) and blue (400-450 nm), and reflection in the green (495-570 nm). The two components of chlorophyll (a and b) were also mainly contributing to the red/NIR region (600-750 nm), and the main contributing bands for chl b shifted towards green comparing to those for chl a (Fig. 6b and 6c) (Ustin et al. 2009). Carotenoids have a similar VIP curve comparing with the chlorophyll, with one distinction: the VIP values for carotenoids between 650 nm and 700 nm are relatively higher to those of chlorophyll.

376 Comparing with the pigments, N_{mass}, C_{mass} and LMA have relatively smooth VIP
377 curves. For N_{mass}, wavelengths around 700 nm and beyond 1900 nm are important to the
378 prediction of N_{mass}, presumably because the visible region is controlled by pigments and
379 nitrogen is an important component in leaf pigments, and the SWIR region near 2000 nm
380 is controlled by protein absorption features (Kokaly et al. 2009). Both C_{mass} and LMA
381 were related to the leaf structure and were largely contributing to the reflectance at NIR
382 and SWIR.

383 3.4. Robustness of the PLSR approach across time, sites and light environment

384 We examined the performance of the $PLSR_{ref}$ models under five scenarios where
385 different sampling strategies were applied. The performance of the PLSR models
386 generally improved in the order of spring, fall, summer, monthly, and biweekly (Table 4).
387 As expected, more sampling throughout the season (and the increasing size and
388 representativeness of the calibration dataset) increased R^2 and reduced RMSE. When
389 comparing the three seasons, summer-only sampling yielded higher model performance
390 relative to the other two seasons, yet the improvements from scenarios 2 (summer-only)
391 to monthly (scenario 4) were not as obvious for pigments as much as N_{mass}, C_{mass} and
392 LMA. Sampling biweekly (scenario 5) largely improved the performance of PLSR,
393 especially for N_{mass} and C_{mass} (R^2 increased from <0.4 to ~0.6).

394 Examining the seasonal patterns of predicted and observed leaf traits reveal time-
395 dependent performance of each scenario. In spring-only scenario where leaf samples only
396 from the spring were used for PLSR calibration, all leaf traits during the first four weeks
397 of the growing seasons were well estimated. However, fall season leaf traits were
398 overestimated except for LMA in Martha's Vineyard (Fig. S4m). By contrast, in the fall-

399 only scenario, spring and summer leaf traits were underestimated except for C_{mass} (Fig.
400 S5k). Our summer-only scenario showed a better ability to capture the seasonal patterns
401 of leaf traits, only underestimated the N_{mass} peak in the early spring at Harvard Forest
402 (Fig. S6j). The monthly sampling scenario improved estimation of all leaf traits, in which
403 the improvement on estimating LMA was the most obvious (R^2 from 0.26 in the summer
404 case to 0.76 in the monthly sampling case, Fig. S7m, S7n). Biweekly sampling scenario
405 appeared to produce a satisfactory result for all the leaf traits studied here (Fig. S8).

406 $PLSR_{ref}$ models trained using sunlit leaves explain 35%-70% of the variability in
407 shaded leaves with highest R^2 for pigments while lowest R^2 for C_{mass} (Fig. S9, Table S1).
408 However, $PLSR_{ref}$ was less accurate for leaf traits like LMA in terms of RMSE (Fig.
409 S10m), for which the difference between sun-lit and shaded leaves was significant (Fig.
410 2). Similarly, $PLSR_{ref}$ models trained with shaded leaves were able to predict the sunlit
411 leaf traits, but with lower model performance compared to when trained with sunlit
412 foliage. Depending on the leaf traits, the variability explained by PLSR ranges from 35%
413 to 70% (Fig. S10m).

414 $PLSR_{ref}$ models trained using data from Harvard Forest (Test 1) were able to
415 capture 60~70% of variability of the pigments from Martha's Vineyard, except for N_{mass}
416 and C_{mass} (Table 5). Similar results were obtained from $PLSR_{ref}$ trained using Martha's
417 Vineyard data (Test 2) and validated with HF data. VIP values for pigments in Test 1
418 were similar to those from Test 2. This is in stark contrast with VIP values for Nmass,
419 Cmass, and LMA from both experiments. The locations of important wavelengths were
420 quite different between two tests (Fig. S11).

421 **Table 4** Performance of all scenarios (spring, summer, fall, monthly, and biweekly) in terms of the goodness-of-fit (RMSE, R^2)
422

Leaf traits	RMSE					R^2				
	Spring	Summer	Fall	Monthly	Biweekly	Spring	Summer	Fall	Monthly	Biweekly
Total Chl ($\mu g/cm^2$)	8.64	6.64	7.23	6.32	5.66	0.60	0.70	0.72	0.73	0.77
Chl a ($\mu g/cm^2$)	5.97	4.75	5.25	4.65	4.15	0.63	0.72	0.72	0.73	0.78
Chl b ($\mu g/cm^2$)	2.73	1.92	2.06	1.89	1.69	0.48	0.67	0.69	0.69	0.73
Car ($\mu g/cm^2$)	1.71	1.31	1.29	1.22	1.12	0.48	0.65	0.69	0.69	0.73
N_{mass} (%)	1.62	0.42	0.51	0.37	0.29	0.08	0.36	0.07	0.36	0.62
C_{mass} (%)	1.59	1.71	1.74	1.26	1.03	0.20	0.21	0.19	0.39	0.56
LMA (g/cm^2)	61.13	27.17	24.86	21.78	18.76	0.13	0.71	0.75	0.79	0.85

Table 5 Performance of PLSR reflectance models that were calibrated using data from one site and validated using data from the other site.

Leaf traits	RMSE		R^2	
	MV→HF	HF→MV	MV→HF	HF→MV
Total Chl ($\mu g/cm^2$)	6.17	7.44	0.72	0.67
Chl a ($\mu g/cm^2$)	4.39	5.29	0.73	0.69
Chl b ($\mu g/cm^2$)	1.85	1.99	0.68	0.66
Car ($\mu g/cm^2$)	1.19	1.54	0.59	0.59
$\mathbf{N_{mass}}$ (%)	0.56	0.72	0.29	0.20
$\mathbf{C_{mass}}$ (%)	2.89	2.90	0.10	0.23
LMA (g/cm^2)	35.62	59.45	0.60	0.72

4. Discussion

4.1 Can we track the seasonality of leaf traits using leaf spectroscopy?

Here we show that the seasonal variability of leaf traits can be captured with leaf spectroscopy approaches (Fig.5, Table 3). All leaf properties (seven leaf traits and leaf spectra) display seasonal dynamics that are also related to the location and microclimate (i.e., sunlit vs. shaded, and the accompanying changes in humidity and temperature). The PLSR approach explained 60%~80% of variability of these leaf traits in our study, supporting the hypothesis that leaf spectra can capture the seasonal variability of leaf traits. Indeed, each leaf trait has its own spectral fingerprint, as we have seen from the VIP values of PLSR models (Fig.7). Patterns of VIP values were similar to previous studies (Asner et al. 2009; Serbin et al. 2014) and consistent with our understandings of leaf physiology (Ustin et al. 2009). This is an important result as collecting leaf spectra is much more time-efficient than traditional approaches and allows for repeat sampling of the same leaves throughout the season. SVIs can be an alternative for the estimation of total chlorophyll concentration when there are limits on available instruments or, for example, using two-band LED sensors (e.g., Garrity et al. 2010; Ryu et al. 2010). The result also has implications for the current and future use of field spectrometers that measure leaf or canopy reflectance at high temporal frequency (e.g., Hilker et al. 2009). Our well-calibrated model using PLSR can be used on leaf reflectance to track the seasonality of multiple leaf traits in temperate deciduous forests.

The tests on the robustness of leaf spectra-trait relationships suggested that the overlap between the training dataset and an independent validation dataset is important for a good prediction. Summer mature leaves displayed higher pigments concentration and LMA, while

lower N_{mass} compared with young leaves (Fig. 1, Fig. 2). In addition, the corresponding leaf spectra were significantly different (Fig. 4). Traditionally, the development of the leaf traits-spectra relationship has been focused on a single time point, typically mid-season mature leaves. We have shown here that if we apply an empirical relationship between spectra and traits derived from one period (for example, summer) to another (spring or fall), leaf traits will likely be over or under-estimated (Fig. S4-S6). Thus predicting leaf traits like N_{mass}, which has an obvious seasonality, will not be well represented. However, we have also illustrated that with proper calibration, we can adequately characterize the seasonality of a range of leaf traits, which is critical for ecosystem monitoring and informing process modeling activities (Table 5).

VIP values as indictors of band importance can help to explain the prediction power of PLSR models. For example, in the case of using PLSR trained use data from one site to predict another (Test 1 & 2), VIP values of leaf pigments overlap well, indicating both sites share similar wavelength regions (Fig. S11). As a result, cross-site prediction of leaf pigments showed reasonable accuracy (Table 5). It also has important implications for the design of multi-band sensors and imagers as it can select the wavelengths that are most useful for the leaf traits of interest (Nijland et al. 2014; Ryu et al. 2010).

The variability of our seven leaf traits was not equally captured (Table 3). The absorption features of pigments are well understood and clearly represented in the VIP value plots (Fig. 6). While for C_{mass} and N_{mass}, although there have been studies on the possible linkage between certain components in the leaves (e.g., protein, cellulose) and leaves' optical properties, the impact on leaf spectra is less obvious comparing with that from the pigments (Kokaly et al., 2009). This may partly explain the less accurate PLSR models for the C_{mass} and N_{mass}.

As expected, the PLSR approach, which can exploit the full spectrum information to estimate leaf traits performed better than traditional SVIs (Table 3). While SVIs that calibrated with extensive datasets displayed a similar performance to PLSR in estimating total chlorophyll concentration, we observed significant difference for the carotenoids and LMA. Recalibrate SVIs using our own datasets did not improve their performance. This suggests that the leaf traits variability in our dataset was not fully captured by the SVIs, despite that our large dataset covers ranges observed by others (Féret et al. 2011). Incorporating more datasets to the calibration of simple indices could potentially improve the performance of these methods, but will not alleviate the saturation issue that is pervasive when using simple SVIs, especially for LMA.

As the applications of leaf spectra-traits relationship become more common, we argue that a standardized protocol to calibrate and validate PLSR-type models is needed. This includes an independent validation dataset to avoid validating against the calibration dataset itself and a method to choose the optimal number of PLSR components to prevent overfitting (Serbin et al. 2014). A globally relevant algorithm for leaf traits that can be used by ground spectral observations (Hilker et al. 2010) or existing or planned satellite missions like HyspIRI (such as https://hyspiri.jpl.nasa.gov/) hinges on a rigorously-tested method and on datasets covering a wide range of variations in leaf traits.

4.2 The implications for field sampling strategy

The leaf traits time-series we presented showed the critical time windows to capture their seasonality. Extensive field sampling is laborious and expensive and the continual question in plant ecology is “how much is good enough?” Since the measurements of leaf spectral properties are less labor-intensive (and non-destructive) compared with the measurements of most leaf traits,

494 we explored how many destructive measurements of leaf traits were needed to calibrate the
495 models using full leaf spectra. For example, LMA showed dramatic changes in the early season,
496 thus the sampling and calibration processes need to include the data at this stage. Similarly, N_{mass}
497 was relatively stable in the mid season, and most of the variations occurred in the early and end
498 of season, which makes the sampling at these time frames important. This explains why our
499 comparisons that only considered the variability of leaf traits in the summer showed much poorer
500 performance. Monthly and even biweekly sampling should be considered, at least for the four
501 temperate deciduous species examined in this study.
502
503 *4.3 Broad implications of using leaf spectroscopy for ecological studies*
504 Understanding the seasonality of leaf traits has recently gained attention as an effort to
505 improve our modeling of terrestrial carbon and water cycles (Bauerle et al. 2012; Grassi et al.
506 2005; Medvigy et al. 2013). For example, in the Community Land Model, N_{mass} and LMA
507 control the maximum rate of carboxylation, V_{cmax}, which is highly variable temporally and
508 across different species and light environments (Oleson et al., 2010). Our time-series of N_{mass}
509 capture two important features: (1) the seasonal peak at the beginning of the spring, suggesting
510 that nitrogen was allocated to the leaves early in the season. As leaves matured, other types of
511 elements such as carbon accumulated at a faster rate, resulting in an increase of C_{mass} relative to
512 N_{mass} ratio. (2) A decline of N_{mass} by the end of the season. N_{mass} and LMA was relatively stable
513 at both sites during the summer (Fig. 2a and 2b), thus leaf age does not appear to be affecting the
514 nitrogen concentration during the peak season (Field and Mooney 1983). This finding highlights
515 the importance of tracking the seasonality of leaf traits (Wilson et al. 2000), and our work
516 demonstrates that leaf spectroscopy can provide a rapid means to routinely measure leaf traits.

Importantly, these results highlight that spectroscopy observations can provide key information on the individual differences in multiple leaf traits that can feed into ecosystem models (Medvigy et al., 2009) or be used to test key ecological questions (Rowland et al., 2015). In addition, this emphasizes the important capability of monitoring ecosystem dynamics across a range of spatial and temporal scales with hyperspectral observations from leaves, towers, as well as with new instruments mounted on Unmanned Aerial Systems (UASs) and existing and future instruments on piloted aircraft and satellite platforms (Yang et al., 2014; Yang et al., 2015; Asner and Martin, 2008; Hilker et al., 2010).

5. Conclusion

This paper presents a comprehensive study of the relationship between leaf spectra and foliar traits across varying leaf developmental stages, sites, and light environment using a near weekly dataset of seven leaf traits and spectra at two sites. A Partial Least Square Regression (PLSR) modeling approach, after proper calibration with leaf traits from different times of the season, showed a strong capacity to quantify the seasonal variation of leaf traits within and across sites. The robustness of a PLSR model largely depends on the overlap of leaf trait ranges between the calibration dataset and the dataset to be estimated, and extrapolation outside the ranges of the calibration dataset can result in a significant error. We found that biweekly sampling of leaf traits and spectra would provide a robust PLSR model to estimate the seasonal variations of leaf traits. This work demonstrated the capability of leaf spectra to track seasonally-variable leaf traits, and thus supports the use of automated field spectrometers, airborne and satellite hyperspectral sensors to track leaf traits repeatedly throughout the season and across broad regions (Roberts et al. 2012; Singh et al., 2015; Yang et al. 2015).

Acknowledgements

We thank Katie Laushman, Lakiah Clark, Skyler Hackley, Rui Zhang, Kate Morkeski, Mengdi Cui, Marc Mayes and Tim Savas for assisting with fieldwork. We thank Matthew Erickson, Marshall Otter, Rich McHorney, Jane Tucker and Sam Kelsey from the Marine Biological Laboratory for the help with labwork. We also thank the Harvard Forest, the Manuel F. Correllus State Forest, Nature's Conservancy Hoft Farm Preserve and Mr. Colbert for the permission to use the forests for research. This research was supported by the Brown University–Marine Biological Laboratory graduate program in Biological and Environmental Sciences, and Marine Biological Laboratory start-up funding for JT. JT was also partially supported by the U.S. Department of Energy (U.S. DOE) Office of Biological and Environmental Research grant DE-SC0006951 and the National Science Foundation grants DBI-959333 and AGS-1005663. SPS was supported in part by the U.S. DOE contract No. DE-SC00112704 to Brookhaven National Laboratory. JW was supported by the NASA Earth and Space Science Fellowship (NESSF2014).

Reference

Asner, G., & Martin, R. (2008). Spectral and chemical analysis of tropical forests: Scaling from leaf to canopy levels. *Remote Sensing of Environment, 112,* 3958-3970

Asner, G.P., Martin, R.E., Ford, A., Metcalfe, D., & Liddell, M. (2009). Leaf chemical and spectral diversity in Australian tropical forests. *Ecological Applications, 19,* 236-253

Asner, G.P., Martin, R.E., Knapp, D.E., Tupayachi, R., Anderson, C., Carranza, L., Martinez, P., Houcheime, M., Sinca, F., & Weiss, P. (2011). Spectroscopy of canopy chemicals in humid tropical forests. *Remote Sensing of Environment, 115,* 3587-3598

567 Asner, G.P., & Vitousek, P.M. (2005). Remote analysis of biological invasion and
568 biogeochemical change. *Proc Natl Acad Sci U S A, 102*, 4383-4386

569 Bauerle, W.L., Oren, R., Way, D.A., Qian, S.S., Stoy, P.C., Thornton, P.E., Bowden, J.D.,
570 Hoffman, F.M., & Reynolds, R.F. (2012). Photoperiodic regulation of the seasonal pattern of
571 photosynthetic capacity and the implications for carbon cycling. *Proceedings of the National*
572 *Academy of Sciences, 109*, 8612-8617

573 Belanger, M., Miller, J., & Boyer, M. (1995). Comparative relationships between some red edge
574 parameters and seasonal leaf chlorophyll concentrations. *Canadian Journal of Remote Sensing,*
575 *21*, 16-21

576 Bonan, G.B., Oleson, K.W., Fisher, R.A., Lasslop, G., & Reichstein, M. (2012). Reconciling leaf
577 physiological traits and canopy flux data: Use of the TRY and FLUXNET databases in the
578 Community Land Model version 4. *Journal of Geophysical Research: Biogeosciences, 117*,
579 G02026.

580 Chapin, F.S., Matson, P.A., & Vitousek, P.M. (2011). *Principles of terrestrial ecosystem*
581 *ecology*. (2nd Edition ed.). Springer

582 Couture, J.J., Serbin, S.P., & Townsend, P.A. (2013). Spectroscopic sensitivity of real-time,
583 rapidly induced phytochemical change in response to damage. *New Phytologist*, 198, 311-319.

584 Curran, P.J. (1989). Remote sensing of foliar chemistry. *Remote Sensing of Environment, 30*,
585 271-278

586 Demmig-Adams, B., & Adams, W.W. (2000). Photosynthesis: Harvesting sunlight safely.
587 *Nature, 403*, 371-374

588 Dillen, S.Y., de Beeck, M.O., Hufkens, K., Buonanduci, M., & Phillips, N.G. (2012). Seasonal
589 patterns of foliar reflectance in relation to photosynthetic capacity and color index in two co-
590 occurring tree species, Quercus rubra and Betula papyrifera. *Agricultural and Forest*
591 *Meteorology, 160*, 60-68

592 Eckstein, R.L., Karlsson, P.S., & Weih, M. (1999). Leaf life span and nutrient resorption as
593 determinants of plant nutrient conservation in temperate-arctic regions. *New Phytologist, 143*,
594 177-189

595 Ellsworth, D.S., & Reich, P.B. (1993). Canopy structure and vertical patterns of photosynthesis
596 and related leaf traits in a deciduous forest. *Oecologia, 96*, 169-178

597 Elvidge, C.D. (1990). Visible and near infrared reflectance characteristics of dry plant materials.
598 *International Journal of Remote Sensing, 11*, 1775-1795

599 Evans, J. (1989). Photosynthesis and nitrogen relationships in leaves of C3 plants. *Oecologia, 78*,
600 9-19

601 Evans, J. (1989b). Partitioning of nitrogen between and within leaves grown under different
602 irradiances. *Australian Journal of Plant Physiology* 16(6): 533-548.

603 Féret, J.-B., François, C., Gitelson, A., Asner, G.P., Barry, K.M., Panigada, C., Richardson,
604 A.D., & Jacquemoud, S. (2011). Optimizing spectral indices and chemometric analysis of leaf
605 chemical properties using radiative transfer modeling. *Remote Sensing of Environment, 115*,
606 2742-2750

607 Field, C., & Mooney, H.A. (1983). Leaf age and seasonal effects on light, water, and nitrogen
608 use efficiency in a California shrub. *Oecologia, 56*, 348-355

609 Fisher, J., & Mustard, J. (2007). Cross-scalar satellite phenology from ground, Landsat, and
610 MODIS data. *Remote Sensing of Environment, 109*, 261-273

611 Foster, D., Hall, B., Barry, S., Clayden, S., & Parshall, T. (2002). Cultural, environmental and
612 historical controls of vegetation patterns and the modern conservation setting on the island of
613 Martha's Vineyard, USA. *Journal of Biogeography, 29*, 1381-1400

614 Garrity, S.R., Vierling, L.A., & Bickford, K. (2010). A simple filtered photodiode instrument for
615 continuous measurement of narrowband NDVI and PRI over vegetated canopies. *Agricultural*
616 *and Forest Meteorology, 150*, 489-496

617 Grassi, G., Vicinelli, E., Ponti, F., Cantoni, L., & Magnani, F. (2005). Seasonal and interannual
618 variability of photosynthetic capacity in relation to leaf nitrogen in a deciduous forest plantation
619 in northern Italy. *Tree Physiol, 25*, 349-360

620 Hilker, T., Coops, N.C., Coggins, S.B., Wulder, M.A., Brownc, M., Black, T.A., Nesic, Z., &
621 Lessard, D. (2009). Detection of foliage conditions and disturbance from multi-angular high
622 spectral resolution remote sensing. *Remote Sensing of Environment, 113*, 421-434

623 Hilker, T., Nesic, Z., Coops, N.C., & Lessard, D. (2010). A New, Automated, Multiangular
624 Radiometer Instrument for Tower-Based Observations of Canopy Reflectance (Amspec Ii).
625 *Instrumentation Science & Technology, 38*, 319-340

626 Huete, A., Didan, K., Miura, T., Rodriguez, E.P., Gao, X., & Ferreira, L.G. (2002). Overview of
627 the radiometric and biophysical performance of the MODIS vegetation indices. *Remote Sensing*
628 *of Environment, 83*, 195-213

629 Jacquemoud, S., & Baret, F. (1990). PROSPECT: A model of leaf optical properties spectra.
630 *Remote Sensing of Environment, 34*, 75-91

631 Kattge, J., Díaz, S., Lavorel, S., Prentice, I.C., Leadley, P., Bönisch, G., Garnier, E., Westoby,
632 M., Reich, P.B., Wright, I.J. et al., (2011). TRY - a global database of plant traits. *Global*
633 *Change Biology, 17*, 2905-2935

634 Kennard, R.W., & Stone, L.A. (1969). Computer Aided Design of Experiments. *Technometrics,*
635 *11*, 137-148

636 Killingbeck, K.T. (1996). Nutrients in Senesced Leaves: Keys to the Search for Potential
637 Resorption and Resorption Proficiency. *Ecology, 77*, 1716-1727

638 Kokaly, R.F., Asner, G.P., Ollinger, S.V., Martin, M.E., & Wessman, C.A. (2009).
639 Characterizing canopy biochemistry from imaging spectroscopy and its application to ecosystem
640 studies. *Remote Sensing of Environment, 113*, S78-S91

641 Laisk, A., Nedbal, L., & Govindjee (2009). *Photosynthesis in silico: understanding complexity*
642 *from molecules to ecosystems*. Springer Science & Business Media

643 Lewandowska, M., & Jarvis, P. (1977). Changes in chlorophyll and carotenoid content, specific
644 leaf area and dry weight fraction in Sitka spruce, in response to shading and season. *New*
645 *Phytologist, 79*, 247-256

646 Lichtenthaler, H.K., & Buschmann, C. (2001). Chlorophylls and Carotenoids: Measurement and
647 Characterization by UV-VIS Spectroscopy. *Current Protocols in Food Analytical Chemistry*:
648 John Wiley & Sons, Inc.

649 Medvigy, D., S. C. Wofsy, J. W. Munger, D. Y. Hollinger, and P. R. Moorcroft. (2009)
650 Mechanistic scaling of ecosystem function and dynamics in space and time: Ecosystem
651 Demography model version 2. *Journal of Geophysical Research - Biogeosciences,* 114, G01002,
652 doi:10.1029/2008JG000812.

653 Medvigy, D., Jeong, S.-J., Clark, K.L., Skowronski, N.S., & Schäfer, K.V.R. (2013). Effects of
654 seasonal variation of photosynthetic capacity on the carbon fluxes of a temperate deciduous
655 forest. *Journal of Geophysical Research: Biogeosciences, 118*, 1703-1714

656 Mehmood, T., Liland, K.H., Snipen, L., & Sæbø, S. (2012). A review of variable selection
657 methods in Partial Least Squares Regression. *Chemometrics and Intelligent Laboratory Systems,*
658 *118*, 62-69

659 Niinemets U. 2007**.** Photosynthesis and resource distribution through plant canopies. *Plant Cell*
660 *and Environment* 30(9): 1052-1071.

661 Nijland, W., de Jong, R., de Jong, S.M., Wulder, M.A., Bater, C.W., & Coops, N.C. (2014).
662 Monitoring plant condition and phenology using infrared sensitive consumer grade digital
663 cameras. *Agricultural and Forest Meteorology, 184*, 98-106

664 Oleson, K.W., D.M. Lawrence, G.B. Bonan, et al., 2013: Technical Description of version 4.5 of
665 the Community Land Model (CLM). Ncar Technical Note NCAR/TN-503+STR, National
666 Center for Atmospheric Research, Boulder, CO, DOI: 10.5065/D6RR1W7M.

667 Ollinger, S.V. (2011). Sources of variability in canopy reflectance and the convergent properties
668 of plants. *New Phytologist, 189*, 375-394

669 Poorter, H., Niinemets, Ü., Poorter, L., Wright, I.J., & Villar, R. (2009). Causes and
670 consequences of variation in leaf mass per area (LMA): a meta-analysis. *New Phytologist, 182*,
671 565-588

672 Richardson, A.D., Duigan, S.P., & Berlyn, G.P. (2002). An evaluation of noninvasive methods to
673 estimate foliar chlorophyll content. *New Phytologist, 153*, 185-194

674 Roberts, D.A., Quattrochi, D.A., Hulley, G.C., Hook, S.J., & Green, R.O. (2012). Synergies
675 between VSWIR and TIR data for the urban environment: An evaluation of the potential for the
676 Hyperspectral Infrared Imager (HyspIRI) Decadal Survey mission. *Remote Sensing of*
677 *Environment, 117*, 83-101

678 Rowland, L., et al. (2015), Death from drought in tropical forests is triggered by hydraulics not
679 carbon starvation, *Nature*, *528*(7580), 119-122, doi:10.1038/nature15539.

680 Ryu, Y., Baldocchi, D.D., Verfaillie, J., Ma, S., Falk, M., Ruiz-Mercado, I., Hehn, T., &
681 Sonnentag, O. (2010). Testing the performance of a novel spectral reflectance sensor, built with
682 light emitting diodes (LEDs), to monitor ecosystem metabolism, structure and function.
683 *Agricultural and Forest Meteorology, 150,* 1597-1606

684 Schimel, D., Pavlick, R., Fisher, J.B., Asner, G.P., Saatchi, S., Townsend, P., Miller, C.,
685 Frankenberg, C., Hibbard, K., & Cox, P. (2015). Observing terrestrial ecosystems and the carbon
686 cycle from space. *Global Change Biology, 21*, 1762-1776

687 Schneider, C.A., Rasband, W.S., & Eliceiri, K.W. (2012). NIH Image to ImageJ: 25 years of
688 image analysis. *Nature Methods, 9*, 671-675

689 Serbin, S.P., Singh, A., McNeil, B.E., Kingdon, C.C., & Townsend, P.A. (2014). Spectroscopic
690 determination of leaf morphological and biochemical traits for northern temperate and boreal tree
691 species. *Ecological Applications, 24*, 1651-1669

692 Shen, M., Chen, J., Zhu, X., & Tang, Y. (2009). Yellow flowers can decrease NDVI and EVI
693 values: evidence from a field experiment in an alpine meadow. *Canadian Journal of Remote*
694 *Sensing*, *35*, 99-106

695 Sims, D.A., & Gamon, J.A. (2002). Relationships between leaf pigment content and spectral
696 reflectance across a wide range of species, leaf structures and developmental stages. *Remote*
697 *Sensing of Environment, 81*, 337-354

698 Singh, A., Serbin, S.P., McNeil, B.E., Kingdon, C.C., & Townsend, P.A. (2015). Imaging
699 spectroscopy algorithms for mapping canopy foliar chemical and morphological traits and their
700 uncertainties. *Ecological Applications*

701 Terashima, I., Miyazawa, S.-I., & Hanba, Y.T. (2001). Why are sun leaves thicker than shade
702 leaves?—Consideration based on analyses of CO2 diffusion in the leaf. *J Plant Res, 114*, 93-105

703 Ustin, S.L., Gitelson, A.A., Jacquemoud, S., Schaepman, M., Asner, G.P., Gamon, J.A., &
704 Zarco-Tejada, P. (2009). Retrieval of foliar information about plant pigment systems from high
705 resolution spectroscopy. *Remote Sensing of Environment, 113*, S67-S77

706 Ustin, S.L., Roberts, D.A., Gamon, J.A., Asner, G.P., & Green, R.O. (2004). Using imaging
707 spectroscopy to study ecosystem processes and properties. *Bioscience, 54*, 523-534

708 Wicklein, H.F., Ollinger, S.V., Martin, M.E., Hollinger, D.Y., Lepine, L.C., Day, M.C., Bartlett,
709 M.K., Richardson, A.D., & Norby, R.J. (2012). Variation in foliar nitrogen and albedo in
710 response to nitrogen fertilization and elevated CO2. *Oecologia, 169*, 915-925

711 Wilson, K.B., Baldocchi, D.D., & Hanson, P.J. (2000). Spatial and seasonal variability of
712 photosynthetic parameters and their relationship to leaf nitrogen in a deciduous forest. *Tree*
713 *Physiol, 20*, 565-578

714 Wofsy, S.C., Goulden, M.L., Munger, J.W., Fan, S.-M., Bakwin, P.S., Daube, B.C., Bassow,
715 S.L., & Bazzaz, F.A. (1993). Net Exchange of CO2 in a Mid-Latitude Forest. *Science, 260*,
716 1314-1317

717 Wold, S., Sjöström, M., & Eriksson, L. (2001). PLS-regression: a basic tool of chemometrics.
718 *Chemometrics and Intelligent Laboratory Systems, 58*, 109-130

719 Wright, I.J., Reich, P.B., Westoby, M., Ackerly, D.D., Baruch, Z., Bongers, F., Cavender-Bares,
720 J., Chapin, T., Cornelissen, J.H.C., Diemer, M., Flexas, J., Garnier, E., Groom, P.K., Gulias, J.,
721 Hikosaka, K., Lamont, B.B., Lee, T., Lee, W., Lusk, C., Midgley, J.J., Navas, M.-L., Niinemets,
722 U., Oleksyn, J., Osada, N., Poorter, H., Poot, P., Prior, L., Pyankov, V.I., Roumet, C., Thomas,
723 S.C., Tjoelker, M.G., Veneklaas, E.J., & Villar, R. (2004). The worldwide leaf economics
724 spectrum. *Nature, 428*, 821-827

725 Yang, X., Mustard, J., Tang, J., & Xu, H. (2012). Regional-scale phenology modeling based on
726 meteorological records and remote sensing observations. *J. Geophys. Res., 117*, G03029

727 Yang, X., Tang, J., & Mustard, J. (2014). Beyond leaf color: comparing camera-based
728 phenological metrics with leaf biochemical, biophysical and spectral properties throughout the
729 growing season of a temperate deciduous forest. *Journal of Geophysical Research:*
730 *Biogeosciences*, 119, 181-191.

731 Yang, X., Tang, J., Mustard, J.F., Lee, J.-E., Rossini, M., Joiner, J., Munger, J.W., Kornfeld, A.,
732 & Richardson, A.D. (2015). Solar-induced chlorophyll fluorescence that correlates with canopy
733 photosynthesis on diurnal and seasonal scales in a temperate deciduous forest. *Geophysical*
734 *Research Letters, 42*, 2977-2987

735 Zhang, Y., Chen, J.M., & Thomas, S.C. (2007). Retrieving seasonal variation in chlorophyll
736 content of overstory and understory sugar maple leaves from leaf-level hyperspectral data.
737 *Canadian Journal of Remote Sensing, 33*, 406-415

738 Zhao, K., Valle, D., Popescu, S., Zhang, X., & Mallick, B. (2013). Hyperspectral remote sensing
739 of plant biochemistry using Bayesian model averaging with variable and band selection. *Remote*
740 *Sensing of Environment, 132*, 102-119